Design and Analysis of Transmission Optical Filter with Multi-FPR Structure for Dense Wavelength Division Multiplexing (DWDM) Communication System

Aseel Abdul Ameer Shakaty
Laser and Optoelectronic Engineering Department, University of Technology/Baghdad
Email: as_eng2006@yahoo.com

Received on: 27/1/2013 & Accepted on: 26/11/2013

Abstract:

In this paper, it is demonstrated by means of simulations, the practical feasibility of a transmission filter implemented from a stack of high and low index birefringent thin films. Simulations were carried out with a software toolbox package implemented as Matlab™ m-files.

The following materials were used (ZnSe, GaAs, BaF2) as coating materials and KB7 glass as substrate material .In this paper it can be study the designing of transmission filter with two ,three or four Fabry- Perot resonators (FPRs) structure .The difference between each one of them show how the number of multi-stack layer belonging to each FPRs affect on the spectral properties of transmission filter and effect on the choosing of coating material on the properties of transmission filter .

Results show that transmission filter of multi- FPRs results in narrowing the transmittance band and making it somewhat flatter at its top from the single one. But if it has multi- FPRs structure with equal length , the band becomes flatter than that of transmission filter with single FPR structure but exhibits some ripples.

The difference between the values of refractive index of multi layer stack has great influence on the transmittance value, the spectral properties and number of peaks in the transmittance spectrum of the transmission filter as shown in the simulated figures.

Keywords: optical transmission filter, antireflection coating, Fabry- Perot resonator (FPR).

تصميم وتحليل مرشحة بصرية نفاذة بتركيبة متعددة إل FPR لمنظومة اتصال متعددة الإرسال فاصلة لأطوال موجية كثيفة

الخلاصة:

في هذا البحث، يتجلى من خلال المحاكاة، تنفيذ الجدوى العملية لمرشحات بصرية نفاذة و الممثلة بحزمة من الاغشية الرقيقة ذات المعامل الانكسار العالية والمنخفضة المصنوعة من المواد ثنائية الانكسار.

وأجريت المحاكاة بمجموعة الأدوات البرمجية المنفذة ضمن ملفات برنامج Matlab. وقد استخدمت المواد التالية في التصميم (ZnSe, GaAs, BaF2) كمواد طلاء و زجاج KB7 كمادة اساس.

في هذه البحث تمت دراسة تصميم مرشحة بصرية نفاذة ذات التركيب المكون من اثنين، ثلاثة او أربعة من مرنان فابري بيروت (FPRs) ، والفرق بين كل واحد منهم . وقد تبين أن عدد الطبقات الثنائية العائدة لكل مرنان يؤثر على الخصائص الطيفية للمرشح النافذ , و تاثير مواد الطلاء المختارة على خصائص ذلك المرشح.
تظهر النتائج أن المرشح الناقل متعدد FPRs له تأثير تقليص نطاق النفاذية وجعلها منبسطة إلى حد ما في قمتها من المرشح الاحادي وإذا كان المرشح لديه بنية متعددة FPRs ذات الطول المتساوي ، فعند ذلك، تصبح الحزمة اكثر انبساطا من تلك التابعة للمرشح الاحادي ولكن تعرض بعض التموجات.
لقد ظهر ان الفرق بين قيم معامل الانكسار في حزمة متعددة الطبقات لديه تأثير كبير على قيمة النفاذية، والخصائص الطيفية وعدد القمم بطيف النفاذية للمرشح البصري و كما موضح في اشكال المحاكاة.

INTRODUCTION:

Higher-order transfer function (HOTF) which represents the relation between the input and output of a linear time-invariant system with zero initial conditions and zero-point equilibrium.[1] For optical imaging devices, as example, it is the Fourier transform of the point spread function or the intensity distribution caused by a point object in the field of view.[2]
HOTF can be used to achieve the broader reflection less notches and in the design of thin-film antireflection coatings, dielectric mirrors, and optical interference filters[3, 4, 5, 6], and in the design of broadband terminations of transmission lines. They are also used in the analysis, synthesis, and simulation of fiber Bragg gratings[7, 8, 9], in the design of narrow-band transmission filters for wavelength-division multiplexing (WDM), and in other fiber-optic signal processing systems[10]. In this paper, we proposed the mathematical modeling of multi-FPR structure .
The main interest in dielectric mirrors is that they have extremely low losses at optical and infrared frequencies, as compared to ordinary metallic mirrors, which can be useful for widely optical device applications.

Theory :

A dielectric mirror (a Bragg reflector) consists of high and low refractive indices, as shown in Fig. (1.A,B)
The optical thicknesses are typically chosen to be quarter-wavelength long, that is, $n_H l_H = n_L l_L = \lambda/4$ at some operating wavelength λ. The standard arrangement is to have an odd number of layers, with the high index layer being the first and last layer. Fig.(1.A) shows the case of nine layers. If the number of layers is M = 2N +1, the number of interfaces will be 2N +2 and the number of media 2N +3. After the first layer, we may view the structure as the repetition of N identical bilayers of low and high indices. The elementary reflection coefficients having the alternative sign as shown in Fig. (1,A) and are given by[11]

$$\rho = \frac{n_H - n_L}{n_H + n_L}, \quad -\rho = \frac{n_L - n_H}{n_H + n_L}, \quad \rho_1 = \frac{n_a - n_L}{n_a + n_L}, \quad \rho_2 = \frac{n_H - n_b}{n_H + n_b} \qquad ...(1)$$

where n_H, n_L, n_a, and n_b are refractive indices for high, low, air and substrate layers, respectively. The substrate n_b can be arbitrary, even the same as the incident medium n_a. In that case, $\rho_2 = -\rho_1$. The reflectivity properties of the structure can be understood by propagating the impedances from bilayer to bilayer. In general case of multi-layer

dielectric slab structure as shown of Figure. (1-B) that's similar to Figure (1-A)but it is more general:[12]
The elementary reflection coefficients ρ_i from the left of each interface are defined in terms of the characteristic impedances or refractive indices as follows:[12]

$$\rho_i = \frac{\eta_i - \eta_{i-1}}{\eta_i + \eta_{i-1}} = \frac{n_{i-1} - n_i}{n_{i-1} + n_i} \quad ,i=1,2,3\ldots\ldots\ldots\ldots\ldots M+1$$

Where $\eta_i=\eta_0/\eta_i$, and the convention $n_0=n_a$ must be used and $n_{m+1}=n_b$, so that $\rho_i=(n_M-n_b)/(n_M-n_b)$ and $1/n_H=\eta_L$.
Therefore the impedance of each boundary is a function of the charecteristics impedance of each low and high layer , so the refractive index of each one is givenas shown below : [12]

$$Z_2 = \frac{\eta_L^2}{Z_s} = \frac{\eta_L^2}{\eta_H^2} Z_4 = \left(\frac{n_H}{n_L}\right)^2 Z_4 = \left(\frac{n_H}{n_L}\right)^4 Z_6 = \left(\frac{n_H}{n_L}\right)^6 Z_8 = \left(\frac{n_H}{n_L}\right)^8 \eta_b \qquad .....(2)$$

Therefore, after each bilayer, the impedance decreases by a factor of $(n_L/n_H)^2$. After N bilayers, we will have
$Z_2=\left(\frac{n_H}{n_L}\right)^{2N} \eta_b$.

Using $Z_1=\frac{\eta_H^2}{Z_s}$,the reflection response at λ_0 is given by [13]

$$\Gamma_1 = \frac{Z_1 - r_s}{Z_1 + r_s} = \frac{1 - \left(\frac{n_H}{n_L}\right)^{2N} \frac{n_H^2}{n_b n_s}}{1 + \left(\frac{n_H}{n_L}\right)^{2N} \frac{n_H^2}{n_b n_s}} \qquad ....(3)$$

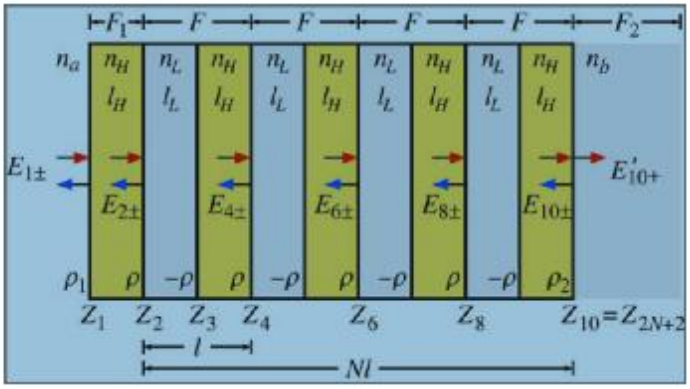

Figure (1-A): Nine-layer dielectric mirror[11]

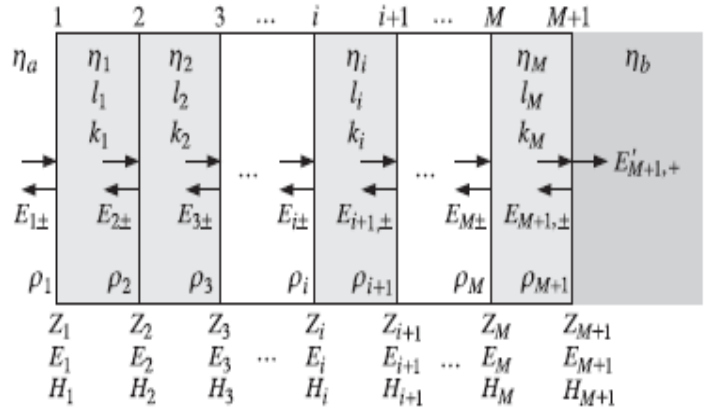

Figure (1-B):Multilayer dielectric slab structure .[12]

It follows that for large N, Γ_1 will tend to −1, that is, 100 % reflection. For nine layers, 2N + 1 = 9, or N = 4, and n_H (ZnS = 2.32) , $n_L(MgF_2)$ = 1.38, and na = nb = 1, we find: $|\Gamma_1|^2$ = 98.84%.[14]

By using the layer recursions, the bandwidth around λ_0 for which the structure exhibits high reflectivity can be determined. Because the bilayers are identical, the forward/backward fields at the left of one bilayer are related to those at the left of the next one by a transition matrix F, which is the product of two propagation matrices of the type of Eq. (2).[11]

The repeated application of the matrix F takes us to the right-most layer.

For example, in Fig.(1-A) we have[12]

$$\begin{bmatrix} E2_+ \\ E2_- \end{bmatrix} = F \begin{bmatrix} E4_+ \\ E4_- \end{bmatrix} = F^2 \begin{bmatrix} E6_+ \\ E6_- \end{bmatrix} = F^3 \begin{bmatrix} E8_+ \\ E8_- \end{bmatrix} = F^4 \begin{bmatrix} E10_+ \\ E10_- \end{bmatrix} \quad \text{.....(4)}$$

where F is the matrix [12]

$$F = \frac{1}{1+\rho} \begin{bmatrix} e^{jl_Lk_l} & \rho e^{-jl_Lk_l} \\ \rho e^{jl_Lk_l} & e^{-jl_Lk_l} \end{bmatrix} \frac{1}{1-\rho} \begin{bmatrix} e^{jl_Lk_l} & \rho e^{-jl_Lk_l} \\ \rho e^{jl_Lk_l} & e^{-jl_Lk_l} \end{bmatrix} \quad \text{.....(5)}$$

Where k_l is the propagation wave number in the low index medium [15]

defining the phase thicknesses $\delta_H = k_H l_H$ and $\delta_L = k_L l_L$, and multiplying the matrix factors out ,we obtain the expression for F by [12]

$$F = \frac{1}{1-\rho^2} \begin{bmatrix} e^{j(\delta_H+\delta_L)} - \rho^2 e^{j(\delta_H-\delta_L)} & -2j\rho e^{-j\delta_H} \sin\delta_L \\ 2j\rho e^{-j\delta_H} \sin\delta_L & e^{-j(\delta_H+\delta_L)} - \rho^2 e^{-j(\delta_H-\delta_L)} \end{bmatrix} \quad \text{.....(6)}$$

The solutions for the left and right band edges and the bandwidth in λ are given by an additional transitional matrix F_1 , we can get to the left interface -1 and additional matrix F_2 ,we can pass to the right of the last interface layer [14]

$$\begin{bmatrix} E_{1+} \\ E_{1-} \end{bmatrix} = F_2 \begin{bmatrix} E_{2+} \\ E_{2-} \end{bmatrix} = F_1 F^4 \begin{bmatrix} E_{10+} \\ E_{10-} \end{bmatrix} = F_1 F_2 F^4 \begin{bmatrix} E_{S+} \\ E_{S-} \end{bmatrix} = F^4 \begin{bmatrix} E_{10+} \\ 0 \end{bmatrix} \quad \text{.....(7)}$$

Where $F_1$and $F_2$are given by

$$F_1 = \frac{1}{\tau_1} \begin{bmatrix} e^{jl_H k_H} & \rho e^{-jl_H k_H} \\ \rho e^{jl_H k_H} & e^{-jl_H k_H} \end{bmatrix}, \quad F_2 = \frac{1}{\tau_2} \begin{bmatrix} 1 & \rho_2 \\ \rho_2 & 1 \end{bmatrix},$$

Where $\tau_1=1+\rho_1$, $\tau_2=1+\rho_2$ in which ρ_1 , ρ_2 were defined in Eq (1). More generally , for 2N+1 layers , or N bilayers , we have

$$\begin{bmatrix} E_{2+} \\ E_{2-} \end{bmatrix} = F^N \begin{bmatrix} E_{2N+2,+} \\ E_{2N+2,-} \end{bmatrix} \quad , \quad \begin{bmatrix} E_{1+} \\ E_{1-} \end{bmatrix} = F_1 F_2 F^N \begin{bmatrix} E_{2N+2,+} \\ 0 \end{bmatrix} \quad \text{.....(8)}$$

Thus , the properties of the multilayer structure are essentially determined by the N^{th} power , F^N ,of the bilayer transition matrix F. In turn, the behavior of F^N is determine by the eigenvalue structure of F.

The eigenvalues $\lambda_{\pm}$ can be both either real or complex value with a unit magnitude . we can represent them in the equivalent form as [14]

$\lambda_+=e^{jkl}$, $\lambda_-=e^{-jkl}$

where l is the length of each bi- layer, $l=l_L+l_H$. the quantity K is referred to as the Bloch wave – number . if the eigen value $\lambda_{\pm}$ are unit magnitude complex values , then K is real . if the eigen values are real values , then K is pure imaginary , say $K = -j\alpha$, so that $\lambda_{\pm} = e^{\pm jkl} = e^{\pm \alpha l}$.

The Eigen values are determined from the characteristic polynomial of F, given by the following expression which is valid from any 2×2 matrix as :[14]

$$\det (F-\lambda I)=\lambda^2 -(\mathrm{tr}F)\,\lambda +\det F$$

where I is the 2×2 identity matrix and trF is the transfers of matrix F . the solution for the left and right band edges and the bandwidth in λ are given by :[14]

$$\lambda_1=\frac{\pi(n_L l_L+n_H l_H)}{\arccos(-\rho)} \quad , \quad \lambda_2=\frac{\pi(n_L l_L+n_H l_H)}{\arccos(\rho)} \quad , \quad \Delta\lambda = \lambda_2-\lambda_1 \quad \text{...(9)}$$

Similarly, the left/right band edges in frequency are $f_1 = c/\lambda_1$ and $f_2 = c/\lambda_2$ as given by [14]

$$f_1= c_0 \frac{\arccos(\rho)}{\pi(n_L l_L+n_H l_H)\arccos(\rho)} \quad , \quad f_2=c_0 \frac{\arccos(-\rho)}{\pi(n_L l_L+n_H l_H)\arccos(-\rho)} \quad \text{...(10)}$$

Noting that from the relationships among the inverse trigonometric functions :[16]

arc cos (-x)= π - arccos (x)

and arc cos(x)=$\frac{\pi}{2}$ - arcsin(x) then arccos(-x) = π – ($\frac{\pi}{2}$ - arcsin(x))

therefore arccos (-ρ) =$\frac{\pi}{2}$ +arcsin(ρ) and arccos(ρ) = π/2 − asin(ρ), then the frequency bandwidth can be written in the equivalent forms as[16]

$$\Delta f = f_2 - f_1 = c_0 \frac{\arccos(-\rho)-\arccos(\rho)}{\pi(n_L l_L+n_H l_H)} = c_0 \frac{2\arcsin(-\rho)}{\pi(n_L l_L+n_H l_H)} \quad \text{...(11)}$$

Relative to some desired wavelength λ= c/f, the normalized bandwidths in wavelength and frequency are given by [17]

$$\frac{\Delta\lambda}{\lambda_0}=\frac{\pi(n_L l_L+n_H l_H)}{\lambda_0}\left[\frac{1}{\arccos(\rho)}-\frac{1}{\arccos(-\rho)}\right] \quad ...(12)$$

$$\frac{\Delta f}{f_0}=\frac{2\lambda_0\arcsin(\rho)}{\pi(n_L l_L+n_H l_H)} \quad ...(13)$$

Similarly, the center of the reflecting band fc = (f1 + f2)/2 is given by[11]

$$\frac{f_c}{f_0}=\frac{\lambda_0}{2(n_L l_L+n_H l_H)} \quad ....(14)$$

If the layers have equal quarter-wave optical lengths at λ_0, that is, $n_H l_H = n_L l_L = \lambda 0/4$, then, fc = f0 and the matrix F takes the simplified form as[16]

$$F=\frac{1}{1-\rho^2}\begin{vmatrix} e^{2j\delta}-\rho^2 & -2j\rho e^{-j\delta}\sin\delta \\ -2j\rho e^{j\delta}\sin\delta & e^{-2j\delta}-\rho^2 \end{vmatrix} \quad ...(15)$$

Where $\delta=\delta_H=\delta_L=2\pi(n_H l_H)/\lambda=(\pi/2)\lambda_n/\lambda=(\pi/2)f/f_0$. Then. Eqs .(12) and (13) are simplified into the form as [14]

$$\frac{\Delta\lambda}{\lambda_0}=\frac{\pi}{2}\left[\frac{1}{\arccos(\rho)}-\frac{1}{\arccos(-\rho)}\right],\ \frac{\Delta f}{f_0}=\frac{4\arcsin(\rho)}{\pi} \quad ...(16)$$

A quarter-wave phase-shifted multilayer structure is obtained by doubling $(HL)^N$to $(HL)^N(HL)^N$ and then inserting a quarter-wave layer L between the two groups,resulting in $(HL)^N L(HL)^N$. We are going to refer to such a structure as a Fabry-Perot resonator (FPR).

A FPR behaves like a single L-layer (layer with low index material) at the design wavelength λ_0. Indeed, noting that at λ_0 the combinations LL and HH(two layer of high index material) are half-wave or absentee layers and can be deleted resulting in the successive reductions . [11]

$(HL)^N L(HL)^N \rightarrow (HL^{(N-1)}HLLHL(HL)^{N-1} \rightarrow (HL)^{(N-1)}HHL(HL)^{(N-1)} \rightarrow (HL)^{(N-1)}L(HL)^{(N-1)}$

Thus, the number of the HL layers can be successively reduced, eventually resulting in the equivalent layer L (at λ_0):[11]

$$(HL)^N L(HL)^N \rightarrow (HL)^{(N-1)}L(HL)^{(N-1)} \rightarrow (HL)^{(N-2)}L(HL)^{(N-2)} \rightarrow \cdots \rightarrow L$$

Adding another L-layer on the right, the structure $(HL)^N L(HL)^N L$ will act as 2L.This structure operate as a half-wave absentee layer at λ_0 [18],If such a structure is sandwiched between the same substrate material, say glass, then it will act as an absentee layer, and it will open up a narrow transmission window at λ_0 in the middle of its reflecting band. [19]

If the quarter-wave layers L are not present, the structures $G|(HL)^N(HL)^N|G$ and $G|(HL)^N|G$ act as mirrors, but with the quarter-wave layers , the structure

$G|(HL)^N L(HL)^N L|G$ acts as a narrow transmission filter, with the transmission bandwidth becoming narrower as N increases[20].

By repeating the FPR $(HL)^N L(HL)^N$ several times and using possibly different Lengths N, it is possible to design a very narrow transmission band centered at λ_0 having a flat pass band and very sharp edges .Such filter designs have been used in thin-film applications and in fiber Bragg gratings, for example , as demultiplexers for WDM systems and for generating very narrow-bandwidth laser sources (typically at λ_0 = 1550 nm) with distributed feedback Lasers. [21]

The varying transmission function of a FPR is induced by interference between the multiple reflections of light between the two reflecting surfaces. Constructive interference occurs if the transmitted beams are in phase, and this corresponds to a high-transmission peak of the etalon. If the transmitted beams are out-of-phase, destructive interference occurs and this corresponds to a transmission minimum. Whether the multiply reflected beams are in phase or not depends on the wavelength (λ) of the light (in vacuum), the angle the light travels through the etalon (θ), the thickness of the etalon (ℓ) and the refractive index of the material between the reflecting surfaces (n).[22]

The phase difference between each succeeding reflection is given by δ:[22]

$$\delta = \frac{2\pi}{\lambda} 2n\ell\cos\theta \qquad \text{....(17)}$$

In which $2n\ell\cos\theta$ is the optical path difference .If both surfaces have a reflectance R, the transmittance function of the etalon is given by[22]

$$T_e = \frac{(1-R)^2}{1-R^2-2R\cos\delta} \qquad \text{.....(18)}$$

$$T_e = \frac{1}{1+F\sin^2(\delta/2)} \qquad \text{....(19)}$$

Where $F = \frac{4R}{(1-R)^2}$

F is the *coefficient of finesse*.

The transmission of an etalon as function of wavelength is shown below in figure (2)[21].

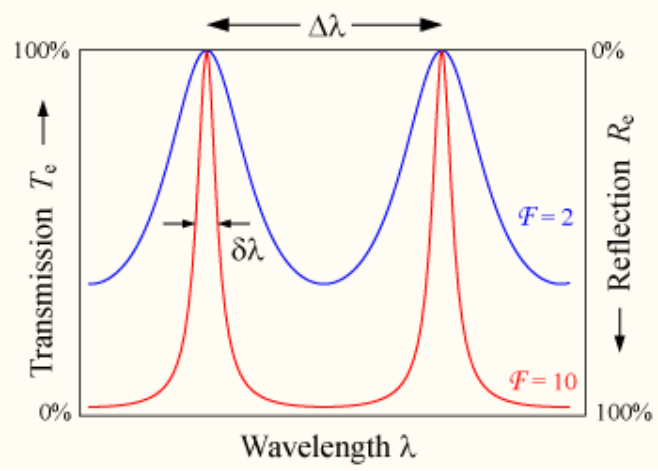

Figure (2):The transmission of an etalon as a function of wavelength, etalon (F=10) shows sharper peaks and lower transmission minima than etalon (F=2).[21]

Maximum transmission (T_e=1) occurs when the optical path length difference (2nl$cos\delta$) between each transmitted beam is an integer multiple of the wavelength.

In the absence of absorption, the reflectance of the etalon R_e is the complement of the transmittance, such that (T_e+R_e)=1. The maximum reflectivity is given by:[22]

$$R_{max}=\frac{4R}{(1+R)^2} \quad \text{.....(20)}$$

Wich occurs when the path-length difference is equal to half an odd multiple of the wavelength.

The wavelength separation between adjacent transmission peaks is called the free spectral range (FSR) of the etalon, Δλ, and is given by:[22]

$$\Delta\lambda=\frac{\lambda_0^2}{2nlcos\theta+\lambda_0} \quad \text{.....(21)}$$

where λ_0 is the central wavelength of the nearest transmission peak. The FSR is related to the full-width half-maximum, δλ, of any one transmission band by a quantity known as the *finesse*:

$$F=\frac{\Delta\lambda}{\delta\lambda}=\frac{\pi}{2asin(1-\sqrt{F})} \quad \text{....(22)}$$

Etalons with high finesse show sharper transmission peaks with lower minimum transmission coefficients.[22]

Some application of transmission filter :

Transmission filter designs have been used in thin-film applications and in fiber Bragg gratings, for example, as demultiplexers for wave division multiplexer WDM systems and for generating very narrow-bandwidth laser sources (typically at λ_0 = 1550 nm) with distributed feedback lasers. [23]

Simulation and result of proposed filter:

The following simulations concern to optical birefringence filters with design wavelength λ_0=1550 nm and the transmittance plotted over the range 1200 nm $\leq \lambda \leq$ 2000 nm.

The structure of the first filter can be represented as follows: $G(HL)^6L(HL)^6$ LG where the exponent numbers represents a layer repetition and G denoted as glass substrate and H is the high refractive index substrate and L is the low refractive index substrate .

In Figure (3) Transmission filter design with in case 1 single FPR filter structure and double FPR filter structure in case 2. This figure illustrates the basic transmission properties of FPR filters such as transmittance band $\Delta\lambda$ that related to, the left totally reflection band edge point λ_1 at which transmittance begun has zero value ,and the right totally reflection band edge point λ_2 at which transmittance just leave zero value .The second properties is the FSR (free spectral range) . Third is the band width value that's related to the full width of half maximum $\delta\lambda$ and finally is the finesse quantity . The parameters chosen that might closely emulate the case of a fiber Bragg grating for dense wavelength division multiplexer DWDM in present applications. The refractive indices of the left and right substrates and the layers for all structure of the design filter are:

$n_a(BK_7$ glass) = n_b = 1.52, $n_L(BaF_2)$ = 1.4693, and n_H (ZnSe)= 2.5. The design wavelength at which the layers are quarter wavelength is taken to be the standard laser source λ_0 = 1550 nm that's taken as normalizing value.

First, comparison between a transmission filter of single FPR structure, which is represent by $G(HL)^{N1}L(HL)^{N1}$ LG with number of stack layers N1 = 6, and transmission filter of double FPRs structure , which is represent by $G|(HL)^{N1}L(HL)^{N1}|(HL)^{N2}L(HL)^{N2}|G$ with N1=6 and N2=6 in the two cases it can be observed the difference between transmission filter of single FPR structure and double FPR structure in transmittance value, FSR value and finesse value and number of fully transmittance peaks as shown clearly in Figure (3) .

It can be observe from Figure (3) that the filter has a suppressed transmittance over the entire reflecting band, where the FPR filter (case 2) has a narrow peak at λ_0=1550 nm with right and left band edge λ1 = 1312nm and λ2 = 1898 nm, the band width $\Delta\lambda$ equal to 586 nm.

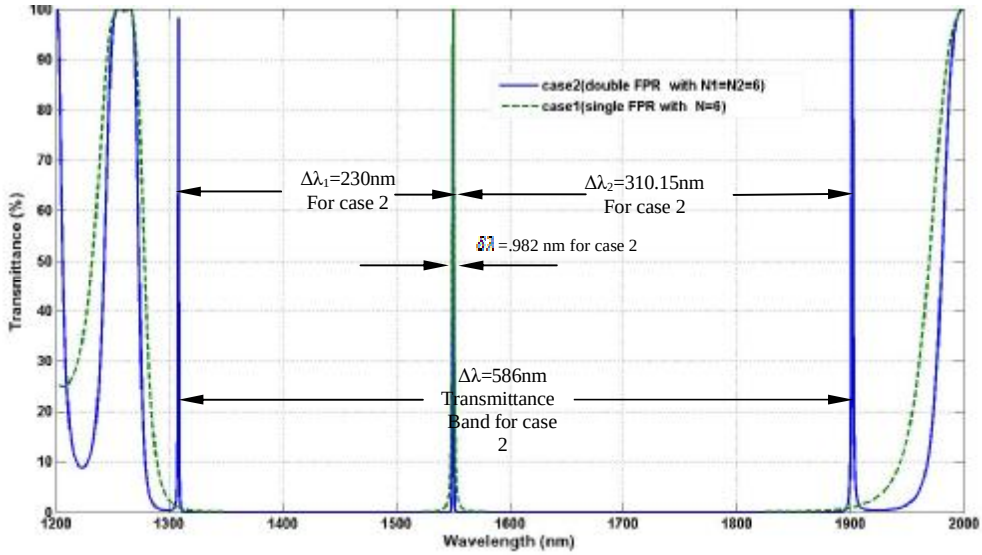

Figure (3) : Transmittance as a function of wavelength of transmission filter (with two cases single FPR structure(N=6) and double FPR structure(N1=N2=6)

The location of the peak can be seen in three position and this is clearly the behavior of optical filter that's used in DWDM the first one is at 1308 nm and the second one is at the design wavelength 1550 and the third one is at 1900 nm and all of them have very narrow peaks with two spectral range value the first one is $\Delta\lambda_1$=230nm and the second one is $\Delta\lambda_2$=310.15 nm , $\delta\lambda$ =0.982 nm, and the finesse value is =596.

The transmittance properties of the single FPR structure filter case (1) of figure (3) is that $\lambda1$ = 1315nm and $\lambda2$ = 1882 nm, the band width of $\Delta\lambda$ is equal to 567 nm. The location of the full transmittance wide peak can be seen in one position at the design wavelength 1550 nm , with two spectral range value the first one is $\Delta\lambda_1$=235nm and the second one is $\Delta\lambda_2$=332 nm , $\delta\lambda$ =1.57 nm, and the finesse value is =318.

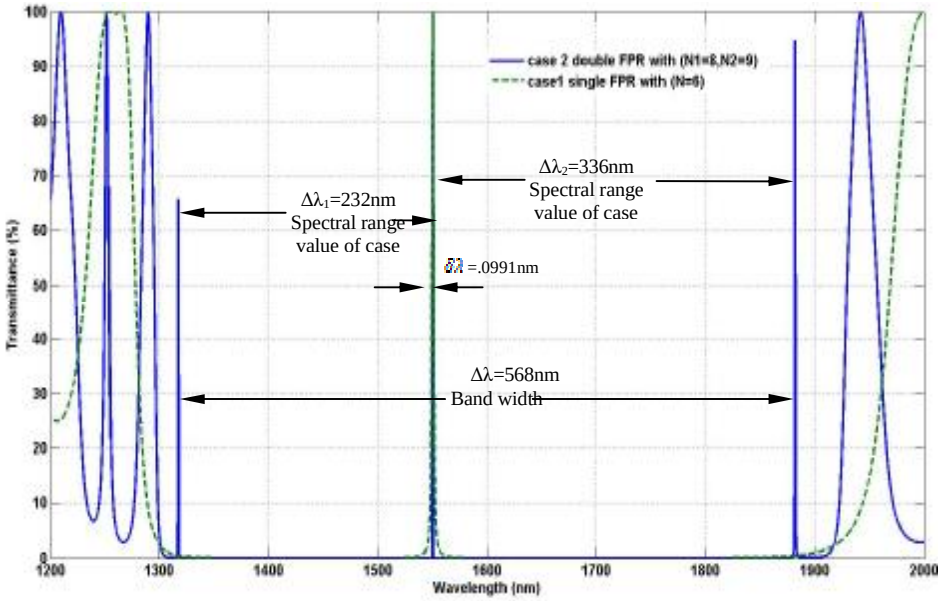

Figure (4): Transmittance as function of wavelength for transmission filter with its spectral properties (with two cases single FPR(N=6) and double FPR (N1=8,N2=9)

In Figure (4) Transmission filter of Figure (3) has been simulated again with different value for the number of stack layer for the double FPR structure (N1=8,N2=9) to study the effect of it on the design filter

It can be observe from Figure (4) that the transmission filter of case 2 has three peaks also at three position (1318nm,1550nm,1886nm) but only one of them at the design wavelength (1550nm) has 100% transmittance value , and it has two spectral range value the first one is $\Delta\lambda_1$=232 nm and the second one is $\Delta\lambda_2$=336 nm , $\delta\lambda$ =0.0991 nm ,with bandwidth value=568nm and the finesse value is =5721.

From the two simulation figures above, it can be seen that, there was difference in the value of transmittance band and spectral range and also the position of peaks and as a result of changing the value of N.

Transmission filters of Figure (4) simulated again with plotting scale from 1549 nm to 1551 nm. Shown in Figure (5) to explain how the value of $\delta\lambda$ calculated from simulation figure and show how the behavior of the transmission filter changed as number of FPR increased.

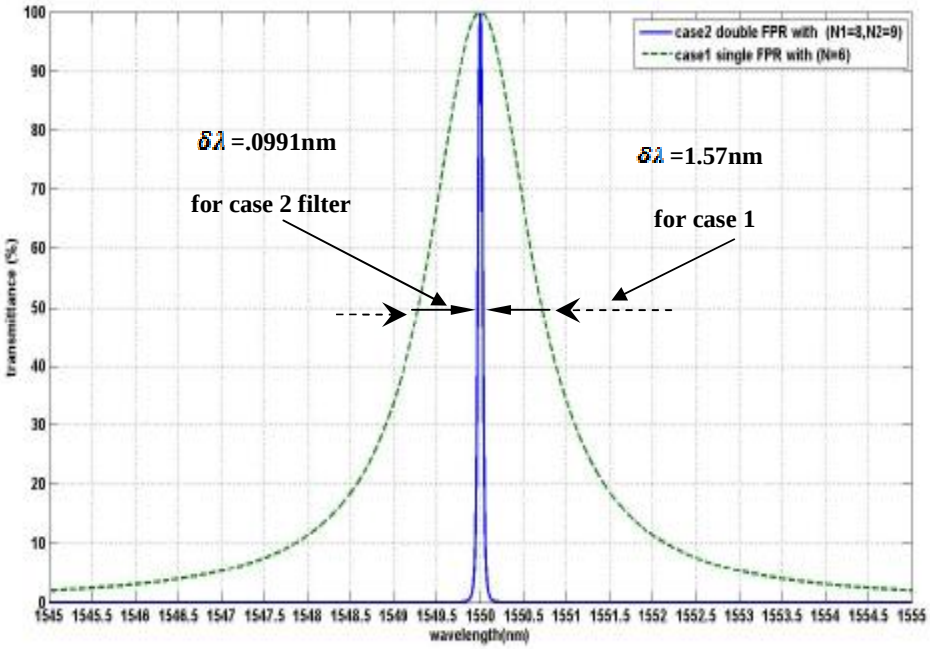

Figure (5): transmittance property of the central peaks at the design wavelength (1550nm) of Figure (4) with different plotting scale.

The resulting transmittance bands are extremely narrow, and became narrower as N increased, Using two FPRs has the effect of narrowing the transmittance band and making it somewhat flatter at its top without ripple and this case happened when (N1=N2) .

To see these bands in the context of the reflectance band transmittance (for N1 = N2 = 8) is plotted on Figure (6) over the range [1549, 1551] nm.

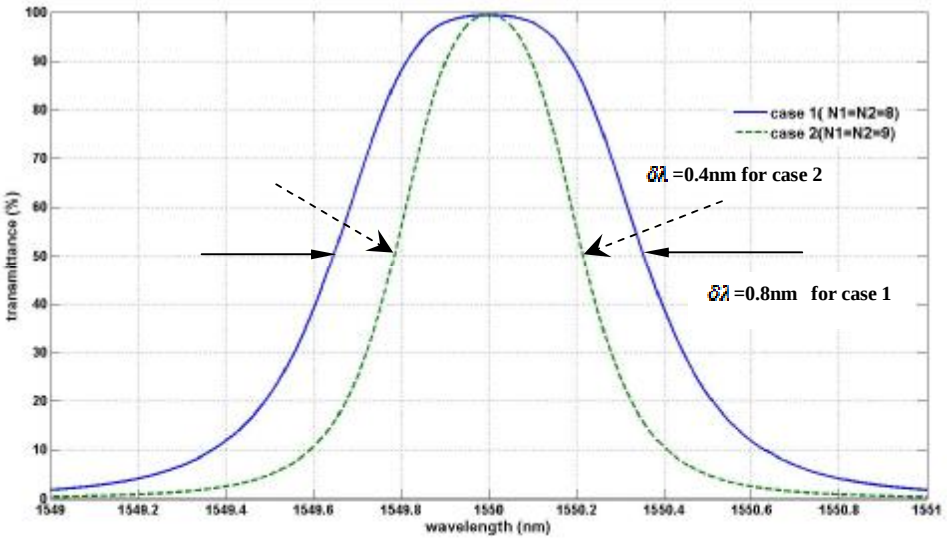

Figure (6): Transmittance as a function of wavelength for central peaks at the design wavelength (1550nm) of two different filter structure with equal stack layer number

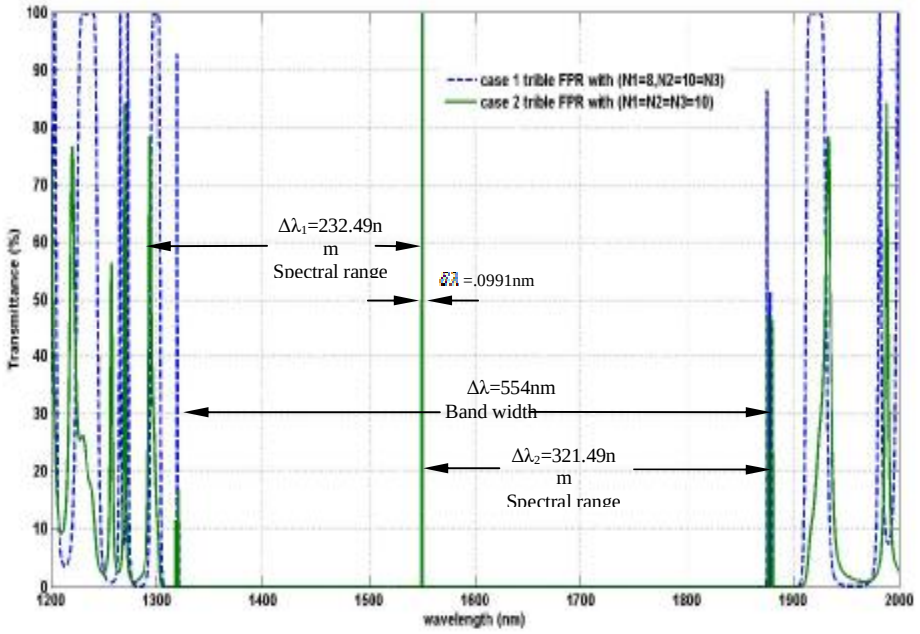

Figure (7): Transmittance as a function of wavelength for transmission filter (two cases of triple FPR structure with different value of stack layer number)

In Figure (6) it can be see that there is two spectral range value for every simulated transmission filter depending on the value of the band edge ,for the first case ($\Delta\lambda_1$=230.4nm for which (λ_1=1319.5nm and λ_2=1549.9) and ($\Delta\lambda_2$=317.91 nm for which λ_1=1550.09nm and λ_2=1868nm) with bandwidth value $\Delta\lambda$=548.5nm, for the second cases the two spectral range is ($\Delta\lambda_1$=232.49nm for which (λ_1=1317.5nm and λ_2=1549.99nm) and $\Delta\lambda_2$=321.49nm for which (λ_1=1550.01nm and λ_2=1871.5nm) with bandwidth value $\Delta\lambda$=554nm, the simulated filter of Figure (7) has three transmittance peaks at three wavelength position depending on its structure , for the first case it is at(1319 nm,1550nm ,1868nm) only one of them has a fully transmittance that's (1550 nm), for the second case it is at(1317.59 nm,1550nm ,1871.59nm) peak at 1550 is only one of them has a fully transmittance.
In order to see the center peaks in clearly form and calculate the value of $\delta\lambda$ easily , the above simulation must be taken again in more suitable scale , as shown clearly in Figure (8) below.

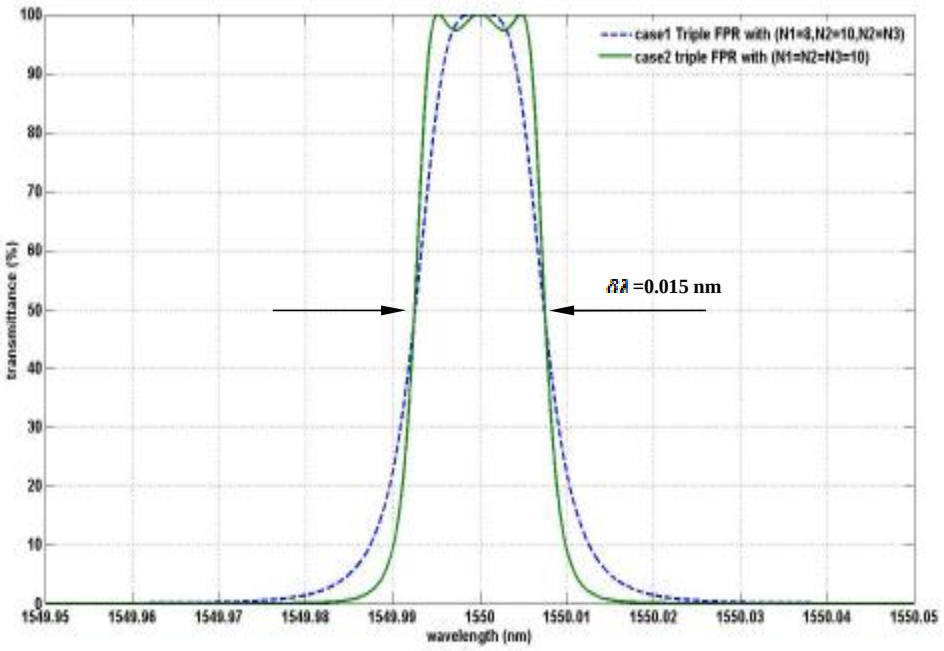

Figure (8): Transmittance as function of wavelength for two different filter of triple FPR structure with different stack layer number for the central peak at the design wave length (1550nm)

From Figure (8) it can be seen that the transmission band is now flatter but exhibits some ripples. To get rid of the ripples, the length of the middle FPR must be slightly increased.
It can be seen also that's the value of $\delta\lambda$ =.015 nm for the two structure.
The fourth FPR filter structure was simulated with two cases for different value of multi stack layer as shown in the Figure (9).

The property of such filter can be obtain from such figure , from the first case the filter has two spectral range band that is ($\Delta\lambda_1$=232.14nm for which (λ_1=1317.85nm and λ_2=1549.99) and ($\Delta\lambda_2$=324.99 nm for which λ_1=1550.01nm and λ_2=1875nm) with bandwidth value $\Delta\lambda$=557.15 nm, for the second cases the two spectral range is ($\Delta\lambda_1$=231.99nm for which (λ_1=1318nm and λ_2=1549.99nm) and $\Delta\lambda_2$=329.49nm for which (λ_1=1550.01nm and λ_2=1879.5nm) with bandwidth value $\Delta\lambda$=561.5nm, the simulated filter of figure 7 has three transmittance peaks at three wavelength position depending on its structure , for the first case it is at(1318 nm,1550nm ,1875nm) peaks at 1550 is only one of 100% transmittance .

It cans be seen also that the peaks became wider than the previous simulated filter ,and this is clearly shown if the scale of Figure (9) expand , as shown in Figure (10).

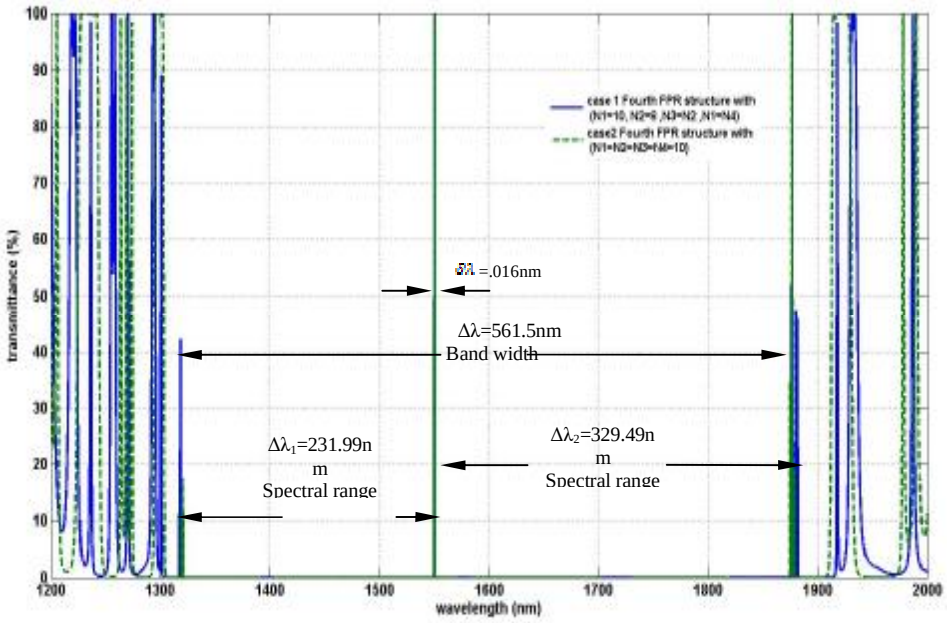

Figure (9): Transmittance as a function of wavelength for transmission filter (two cases of fourth FPR structure with different value of stack layer number).

From Figure (10) it can seen that's the value of $\delta\lambda$ =.014 nm for the first case and $\delta\lambda$ =0.016 nm for the second case , and the ripple of case two increased .

In order to study the effect of changing refractive index difference ($\Delta n=n_H-n_L$) of stack layer on the spectral properties of the transmission filter, different design material have been taken to simulate transmission filter with fourth FPR structure as shown in Figure (11) in which the refractive indices is n_H(GaAs) = 3.41917, and n_L(BaF_2) = 1.4693 ,and n_a=1.52 and n_b=1.52 the design wavelength at which the layers are quarter wavelength is taken to be 1550 nm for the band (1200-2200)nm.

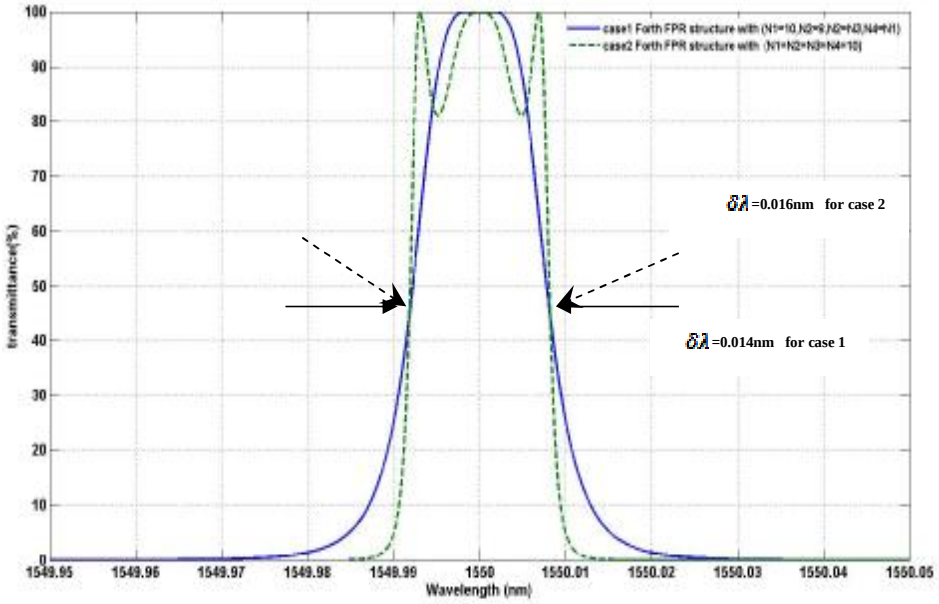

Figure (10) : transmittance as function of wavelength for two different filter of fourth FPR structure with different stack layer number for the central peaks of figure (7).

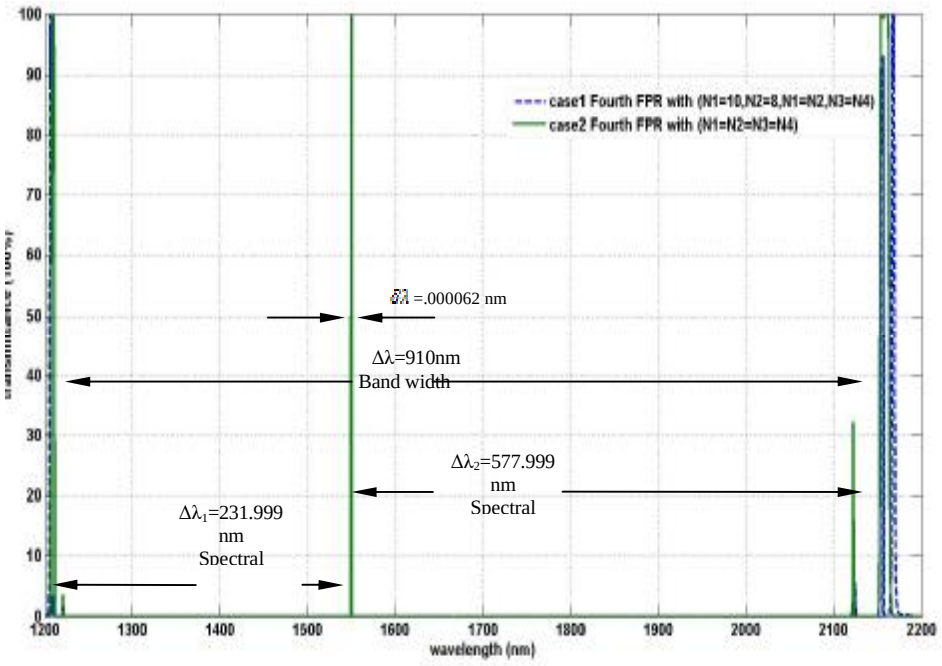

Figure (11): Transmittance as a function of wavelength of a transmission filter for two cases of four FPRs structure

It can be observed from Figure (11) that the value of refractive index of the stack layer of the FPR has great influence on the simulated filter behavior ,broadening the bandwidth and spectral range value for both cases if compare with the cases of figure (9) and made a peaks much wider than that of figure (9) and this notes is true for all simulated filter designed previoslly.

The spectral range value of the first case is ($\Delta\lambda_1$=341.999nm for (λ_1=1208 nm and λ_2=1549.999nm) , $\Delta\lambda_2$=613.999 for ((λ_1=1550.001 nm , λ_2=2164 nm)), $\Delta\lambda$=956nm , and for the second case is ($\Delta\lambda_1$=231.999nm for (λ_1=1218 nm and λ_2=1549.999nm), ($\Delta\lambda$2=577.999nm for (λ_1=1550.001nm and λ_2=2128nm) , $\Delta\lambda$=910nm .

To evaluate the value of $\delta\lambda$ the transmission filter of figure 11 must be simulated again with different scale ,as shown in Figure (12) below, for the first case $\delta\lambda$ =0.000054nm and for the second case $\delta\lambda$=.000062nm

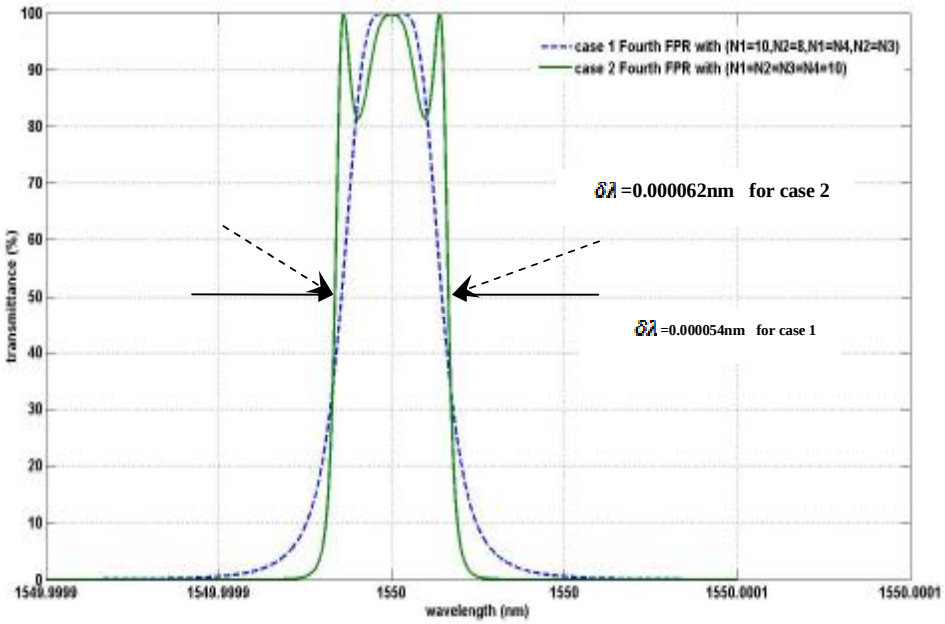

Figure (12) transmittance as function of wavelength for two different filter of fourth FPR structure with different stack layer number for the central peaks of figure (11)

Simulation results and conclusion :

Simulated filters show that:

1- The equal length cases of the simulated filter exhibit ripples, but increasing the length of the middle FPRs tends to eliminate them. The resulting transmittance band is fairly flat and would be appropriate for dense wavelength division multiplexer DWDM systems.

2- Number of antireflection layer (N) affect clearly on the result , and there is great difference between figures of small and large value of N.

3-The refractive index difference ($\Delta n = n_H - n_L$) has great influence on the transmittance value for single design wavelength , and the largest possible value for

suitable type of material is required , for which wide wavelength bandwidth ($\Delta\lambda$) achieved and clearly single wavelength taken with very suitable value of $\delta\lambda$.

4-number of FPR is important point in the design of transmission filter , because its activity on the spectral property of such filter.

5-Because the DWDM uses the same transmission window but with denser channel spacing transmission filter must have many peaks with very small spacing between them that will be effective for making filtering task.

6- Number of "FPR" used inside the structure of transmission filter is very important point in design of it because it is affected directly on the spectral properties of the filter and the number of peaks exist within its transmittance curve.

7- Material used for coating represents another challenge point so it must be chosen carefully according to different specifications that control the design of transmission filter.

8- the transmission filter design above can be used in thin-film applications and in fiber Bragg gratings in optical communication system and for generating very narrow-bandwidth laser sources (typically at λ_0 = 1550 nm) with distributed feedback lasers.

REFERENCES:

[1] Bernd Girod, Rudolf Rabenstein, Alexander Stenger, *Signals and systems*, 2nd ed., Wiley, ISBN 0-471-98800-6 p. 50 ,2001.

[2] The Oxford Dictionary of English, 3rd ed., "higher order Transfer function",2010.

[3] D. Chigrin, A. Lavrinenko, et al. Observation of total omnidirectional reflection from a one-dimensional dielectric lattice. Journal of Applied Physics, 68(A): 25, 1999.

[4] Y. Fink, D. Ripin, et al. Guiding optical light in air using an all-dielectric structure. Journal of Lightwave Technology, 17: 2039,1999.

[5] L. Li, J. Dobrowolski. High-performance thin-film polarizing beam splitter operating at angles greater than the critical angle. Applied Optics, 39: 2754, 2000.

[6] S. Nafisah, H. Hairi, et al. Novel design of multiplexed sensors using a dual FBGs scheme. Microwave and Optical Technology Letters, 52(5): 1218–1221, 2010.

[7] K. Popov, J. Dobrowolski, et al. Broadband high-reflection multilayer coatings at oblique angles of incidence.Applied Optics, 36: 2139, 1997.

[8] T. Saktioto, H. Hairi, et al. Nonlinear parametric studies of photon in a fiber bragg grating. in: 2009 IEEE Symposium on Industrial Electronics and Applications, ISIEA 2009—Proceedings 1, 355–357, 2009.

[9] T. Saktioto, H. Hairi, et al. Nonlinear parametric study of photon in a fibre bragg grating. Physics Procedia,2(1): 81–85.WJMS, 2009.

[10] Mohamed A. Swillam ; Osman S. Ahmed ; Mohamed H. Bakr ; Xun Li . Highly efficient design methodology for very large scale coupled microcavities , *SPIE* 8412, Photonics North 2012 .

[11] T. Saktioto, H. Hairi, et al. Nonlinear parametric studies of photon in a fiber bragg grating. in: 2009 IEEE Symposium on Industrial Electronics and Applications, ISIEA 2009—Proceedings 1, 355–357, 2009.

[12] D. N. Chigrin, A. V. Lavrinenko, D. A. Yarotsky, and S. V. Gaponenko, “Observation of Total Omnidirectional Reflection from a One-Dimensional Dielectric Lattice,” Appl. Phys. A, 68, 25 (1999).

[13] T. Saktioto, H. Hairi, et al. Nonlinear parametric study of photon in a fibre bragg grating. Physics Procedia,2(1): 81–85, 2009.
[14] S. Nafisah, H. Hairi, et al. Novel design of multiplexed sensors using a dual fbgs scheme. Microwave and Optical Technology Letters, 52(5): 1218–1221, 2010.
[15] M. F. Weber, C. A. Stover, L. R. Gilbert, T. J. Nevitt, and A. J. Ouderkirk, "Giant Birefringent Optics in Multilayer Polymer Mirrors," Science, 287, 2451 (2000).
[16] Prof. Sanaullah Bhatti; Ch. Nawab-ud-Din, Ch. Bashir Ahmed, Dr. S. M. Yousuf, Dr. Allah Bukhsh Taheem "Differentiation of Tigonometric, Logarithmic and Exponential Functions". In Prof. Mohammad Maqbool Ellahi, Dr. Karamat Hussain Dar, Faheem Hussain. *Calculus and Analytic Geometry* (in Pakistani English) (First ed.). Lahore: Punjab Textbook Board. p. 140 ,(1999).
[17].Hsi-Chun Liu and Amnon Yariv . Designing coupled-resonator optical waveguides based on high-*Q* tapered grating-defect resonators, Optics Express, Vol. 20, Issue 8, pp. 9249-9263 (2012).
[18] . Guanghui Wang, Perry Ping Shum, Ho-pui Ho, Xia Yu, Dora Juan Juan Hu, Ying Cui, Limin Tong, and Chinlon Lin , Modeling and analysis of localized biosensing and index sensing by introducing effective phase shift in microfiber Bragg grating (μFBG), Optics Express,Vol.19,Issue9,pp.8930-8938(2011).
[19] . Xihua Zou, Fei Wang, and Wei Pan , Flat-top and ultranarrow bandpass filter designed by sampled fiber Bragg grating with multiple equivalent phase shifts,Applied Optics, Vol. 48, Issue4,pp.691-694(2009).
[20] L. Wei and W. Y. Lit, "Phase-Shifted Bragg Grating Filters with Symmetrical Structures," J. LightwaveTechnol., 15, 1405 (1997).
[21] F. Bakhti and P. Sansonetti, "Design and Realization of Multiple Quarter-Wave Phase-Shifts UVWritten Bandpass Filters in Optical Fibers," J. Lightwave Technol., 15, 1433 (1997).
[22] Lipson, S.G.; Lipson, H.; Tannhauser, D.S. *Optical Physics* (3rd ed.). London: Cambridge U.P.. pp. 248. ISBN 0-521-06926-2. (1995).
[23] S. V. Kartalopoulos, Introduction to DWDM Technology, IEEE Press, New York, 2000.